ACS Catalysis

pubs.acs.org/acscatalysis
Research Article

Modeling-Assisted Elucidation of the Organosolv Lignin Depolymerization: Lessons Learned from β-Ether Cleavage over Ni/C

Tina Ročnik Kozmelj, Edita Jasiukaitytė-Grojzdek,* Matej Huš, Miha Grilc,* and Blaž Likozar

Cite This: ACS Catal. 2025, 15, 1182−1194
Read Online

ABSTRACT: The complexity of lignin is a major challenge to overcome in order to develop a complete biorefinery concept for the biobased community. Therefore, the lignin model compound 2-phenoxy-1-phenylethanol was used to design lignin depolymerization. We proposed a two-step mechanism involving predehydrogenation at the C_α-position, removal of the OH group, and subsequent cleavage of the β-*O*-4 bond at the C_β-position into phenol and ethylbenzene. The study was supported by density functional theory and kinetic modeling to evaluate the activation barriers for the cleavage of the β-*O*-4 bond in the dimeric lignin compound. The activation energies for predehydrogenation and cleavage at the C_β-position of phenethoxybenzene were predicted to be 71 kJ mol^{-1} and 9 kJ mol^{-1}, respectively, suggesting that the predehydrogenation is beneficial for the cleavage of the β-*O*-4 bond as it lowers the activation energy. Additionally, the removal of the OH group at the C_α-position increased the reaction rate constant for the β-*O*-4 bond cleavage to 0.68 min^{-1}. By comparing lignin depolymerization and the cleavage of the β-*O*-4 bond in the dimeric lignin compound, the study provided mechanistic insights and suggested process- and structure-dependent correlations. Similarities were found in the process mechanism of aliphatic OH group removal and cleavage at the C_β-position, while the temperature increase contributed more to the enhanced cleavage of the β-*O*-4 bond in the lignin model compound compared to the lignin macromolecule. On the other hand, the reaction conditions affected the structural characteristics of the products after lignin depolymerization, especially the molecular weight and functionality of the oligomeric fragments. We have found that using a lignin model component is beneficial for fundamental research, but correlating the results with the real lignin sample is essential to improve the potential of lignin in the biorefinery concept.

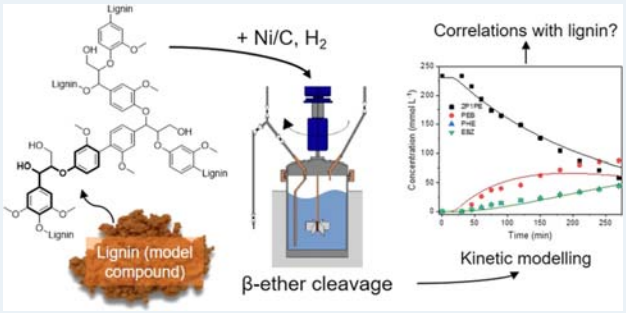

KEYWORDS: *lignin model component, β-ether bond, Ni/C, organosolv lignin, kinetic parameter*

1. INTRODUCTION

Lignin is an aromatic component of lignocellulosic biomass, which has become increasingly important due to its potential as a renewable resource for the production of biofuels, chemicals, and materials. The diverse and complicated nature of lignin poses a major challenge in its valorization and requires a comprehensive understanding of its behavior under different processing conditions.[1−3] The heterogeneity of lignin in terms of chemical structure, dispersity, and molecular weight leads to a variety of multicomponent and multiphase products upon depolymerization, which limits kinetic modeling and the number of compounds in the estimation of kinetic parameters.[4] Kinetic modeling, a powerful tool in the field of chemical engineering and biotechnology, provides a systematic approach to unravel the dynamic processes involved in the lignin depolymerization and conversion.[4−7]

To simplify the determination of kinetic parameters and reduce the complexity and challenges associated with lignin "as is", the lignin model compounds have been introduced into microkinetic studies.[8−10] This approach benefits from the lower complexity, simpler structure, well-characterized, and well-defined lignin moieties and bond types. The β-ether bond (β-*O*-4) is the most common and easy-to-cleave bond type in lignin and therefore a preferred target for cleavage during lignin depolymerization.[11,12] Lignin model compounds facilitate the understanding of the extent of β-ether bond scission and eventually condensation under different conditions.[10,13,14] On the other hand, research should not be limited only to simpler lignin model compounds, since drawing a parallel with real lignin samples is crucial for addressing questions of knowledge transfer of mechanisms and insights so that newly developed approaches can be applied to biorefinery bioplants in the future.[15] Another aspect that needs to be considered

Received: October 2, 2024
Revised: November 29, 2024
Accepted: December 27, 2024
Published: January 6, 2025

https://doi.org/10.1021/acscatal.4c06058
ACS Catal. 2025, 15, 1182−1194

when using lignin model compounds is the variability in the abundance of β-ether bonds within lignin. This variability is significantly influenced by the fractionation methods and the type of biomass feedstock used.[16−18] As a result, the complete process transition from model compounds to lignin is almost impossible to achieve without any process adjustments. Despite these challenges, research into the valorization of lignin model compounds offers valuable insights into the broader context of lignin utilization.[8,15] By identifying correlations between process parameters and the unique structural characteristics of lignin model compounds, researchers gain a more comprehensive understanding of lignin valorization, facilitating the application of this knowledge to the complex and variable environment of real lignin samples. Although process shift is challenging, the study of lignin model compounds serves as a valuable bridge that provides essential insights into lignin valorization strategies that can be optimized based on process- and structure-dependent correlations.[8,10]

Lignin model compounds have provided useful insights into the behavior of lignin under different reaction conditions and have contributed to the development of catalysts and strategies for lignin depolymerization. For instance, the conversion and product distribution of lignin model compounds were particularly influenced by the nature of ether linkages,[19] suggesting a complicated mechanism of lignin depolymerization with nonselective yields of lignin monomers. Jiang et al.[20] synthesized a highly active Ni-based catalyst for the conversion of α-O-4 lignin model compound at near room temperature (30 °C) and mild hydrogen pressure (3 MPa) and further proved the catalyst activity for lignin depolymerization with a monomer yield of 26.6 wt %. Li et al.[21] performed selective hydrodeoxygenation of lignin without changing the reaction pressure with Ni-based carbon-supported composites, whose activity and efficiency were tested on lignin model compounds. Zhang et al.[22] proposed effective hydrogenolysis of lignin model compounds and real lignin at low temperature (100 °C) and low pressure (0.1 MPa) through synergistic effects of NiRu catalyst due to the increased surface atom content, enhanced hydrogen and reactant activation, and inhibited ring hydrogenation. On the other hand, condensation mechanisms between aromatic units mimicking lignin repolymerization were also evaluated using lignin model compounds.[10,14] Although several integrated studies lack the explicit process- and structure-dependent correlation, the clear importance and contribution of lignin model compounds have improved the understanding of lignin depolymerization.

Non-noble metal catalysts are often used for hydrogenation due to their moderate activity and low cost.[22] Among Cu, Fe, and Ni, Ni exhibited the highest catalytic activity and selectivity when lignin model compounds were used for hydrogenation and hydrodeoxygenation.[23] The key catalyst property should be the ability to properly align the adsorbed β-ether compounds to preferentially weaken the carbon−oxygen bonds while avoiding strong binding of the benzene ring to retain aromaticity, which is a challenge in lignin depolymerization that requires a tailored or non-noble catalyst.[24] Therefore, a commercially available Ni/C catalyst was selected for the evaluation of β-ether bond cleavage and lignin depolymerization. Šivec et al.[25] calculated that Ni surface has a mild affinity to bind hydrocarbons at the atomistic level, suggesting that a Ni-based catalyst is beneficial for retaining aromaticity.

This article explores the intricate interplay between lignin structure and kinetic modeling and highlights the mechanistic insights underlying the efficient use of lignin in emerging biobased industries. Through a detailed investigation of reaction kinetics, this study aims to contribute to the development of predictive models that will improve the design and optimization of lignin upgrading processes and ultimately drive the use of this abundant biomass resource.

In our study, 2-phenoxy-1-phenylethanol, a typical lignin model compound with a β-O-4 linkage, was used to mimic the most abundant bond in lignin. The simpler structure of the β-O-4 model compound allowed mechanistic and kinetic aspects of the β-O-4 bond to be investigated with a focus on the intrinsic reactivity of the specific bond. Different operating conditions were applied to investigate the cleavage of the β-O-4 bond by commercially available Ni/C catalyst, while density functional theory (DFT) calculations and kinetic modeling were used to evaluate the bond dissociation energies, as well as the reaction rate kinetics and activation energies required for the defunctionalization and scission of the specific β-ether bond. In addition, the optimal reaction conditions for lignin depolymerization selected from the lignin model compound study were identified using the same experimental setup. The final part of the research aimed to establish process- and structure-dependent correlations relating the operating conditions and the structural similarities between lignin and the lignin model compound. Furthermore, the kinetic parameters determined for the lignin model compound were to be correlated and predicted for the kinetics of lignin depolymerization. The turnover frequencies for the cleavage of β-O-4 bonds were compared. The results of this study will therefore contribute to the development of more efficient strategies for the valorization of lignin.

2. MATERIALS AND METHODS

2.1. Chemicals. The chemicals, solvents, external calibration standards, and gases were used as purchased and were of reagent grade without further purification. Suppliers, purity of chemicals, and CAS numbers are listed in the Supporting Information.

2.2. Hydrogenation of β-Ether Bond. The experiments were performed in a 75 mL multiple reactor system (Series 5000 Multiple Reactor System, Parr Instrument Company, Moline, IL, USA), equipped with a magnetic stirrer. The details and experiments performed are listed in the Supporting Information (Table S1).

2-Phenoxy-1-phenylethanol (2P1PE, 1.75 g) was dissolved in pure ethanol (EtOH) in a ratio of 1:20 (w/v). Experiments were carried out in a temperature range of 175 to 225 °C and hydrogen pressure range of 0.5 to 1.5 MPa for 4 h, loading 5 wt % Ni/C catalyst to achieve 1 wt % nickel on 2P1PE. Liquid samples were taken at 30 min intervals after the reaction mixture had reached the set temperature. The first sample was taken before being heated at room temperature.

2.3. GC−MS Analysis. Samples were analyzed by gas chromatography coupled with mass spectroscopy (GC−MS; Shimadzu, Kyoto, Japan), equipped with an additional flame ionization detector (FID) and a Zebron ZB-5 (Phenomenex, Torrance, CA, USA) capillary column. The concentration of the lignin model component and the identified products were evaluated based on the 7-point calibration using the external standards purchased from Sigma-Aldrich.

2.4. Lignin Depolymerization. The experimental procedure for the depolymerization of ethanol organosolv lignin isolated from beech wood was applied in close accordance with

https://doi.org/10.1021/acscatal.4c06058
ACS Catal. 2025, 15, 1182−1194

the procedure for the lignin model component 2P1PE. Experiments were performed in the temperature range of 175−225 °C and the initially set hydrogen pressure of 1.0 MPa for a period of 4 h. At the end of the reaction time, the reaction mixture was filtered and washed with absolute ethanol to obtain a final volume of 52.5 mL. The filtrate without the mass of the catalyst represents a solid residue (SR). The filtered liquid was used to precipitate the oligomeric fragments (OligF) by adding distilled water in a 3-fold excess. The OligF was collected upon centrifugation, washed repeatedly with distilled water, and freeze-dried. SR and OligF yields were calculated on the basis of the lignin mass.

2.5. Lignin Characterization. Organosolv lignin was analyzed prior depolymerization by size-exclusion chromatography (SEC), 2D heteronuclear single quantum coherence (HSQC) NMR spectra, and quantitative ^{31}P NMR spectra. In addition, oligomeric samples were also analyzed for comparison.

Prior to SEC analysis, the lignin sample was acetylated with pyridine/acetic anhydride following the protocol reported elsewhere.[26] SEC was performed using a size-exclusion chromatographic system (Ultimate 3000, Thermo Fisher Scientific, Massachusetts, USA), equipped with a UV detector at 280 nm, and chromatographic data were processed using PSS WinGPC Unity software. Calibration was performed with polystyrene standards with molecular weights ranging from 672 Da to 127 kDa.

2D-HSQC spectra were recorded using a Bruker AVANCE NEO 600 MHz NMR spectrometer with BBFO probe according to the procedure described by Tran et al.[27] Measurements were conducted in DMSO-d_6, which also served as an internal reference point for the chemical shift (δ_H 2.35 ppm; δ_C 39.5 ppm). Analyses of 2D-HSQC spectra were performed with MestreNova software and following the reported procedure.[26,28]

Quantitative ^{31}P NMR analyses were performed according to the protocol reported by Meng et al.[29] Samples were dissolved in a $CDCl_3$/pyridine mixture (1:1.6), and *N*-hydroxy-5-norbornene-2,3-dicarboxylic acid imide (NHND) was added as an internal standard. 2-Chloro-4,4,5,5-tetramethyl-1,2,3-dioxaphospholane (TMDP) was added to the homogeneous lignin and OligF solution to derivatize the sample. Spectra were recorded with a Bruker AVANCE NEO 600 MHz NMR spectrometer.

3. QUANTUM CALCULATIONS

DFT calculations were carried out using the Gaussian 16 C.02 program suite. A hybrid functional wB97XD, which includes dispersion, was used[30] with the basis set aug-cc-pVTZ.[31] To assess the bond dissociation energy (BDE), the energy of the complete molecule in the relaxed geometry was computed (E_{12}). Second, the two fragments ensuing from the cleavage of a bond in question were separately relaxed, and their energies were computed (E_1, E_2), taking the spin state of the radicals into account. BDE is obtained by eq 1

$$\mathrm{BDE}=E_{12}-E_1-E_2 \tag{1}$$

4. KINETIC MODELING

Hydrogenation of β-*O*-4 lignin model compounds over a Ni/C catalyst under hydrogen atmosphere was carried out in a three-phase system. The kinetic model utilizes the mechanism of the lignin model compound and takes into account the molar balances of the individual components, which are influenced by the mass transfer between the gas phase, the solvent (liquid) phase, and the catalyst surface. In addition, the model takes into account the rates of adsorption, desorption, and reactions occurring at the active sites of the catalyst. The proposed reaction mechanism (Figure 1) was developed based on the

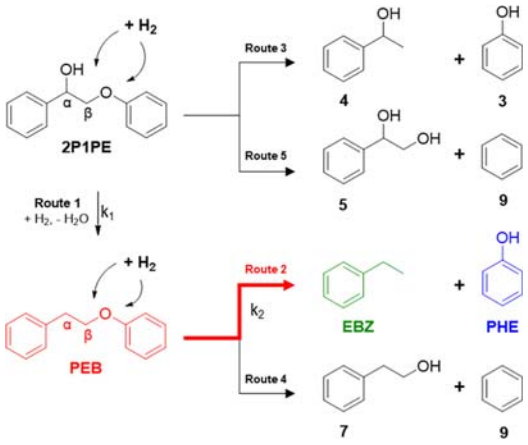

Figure 1. Proposed reaction and cleavage mechanism of β-ether bond over Ni/C catalyst.

intermediates and products identified by analyzing the liquid samples and the theoretical mechanistic principle of possible cleavages within the β-*O*-4 bond. However, only the individual steps of the identified products were incorporated into the kinetic model to determine the kinetic rates of β-*O*-4 bond cleavage of 2-phenoxy-1-phenylethanol. A detailed description of the kinetic model development is available in our previous works.[10,32,33] The key equations for the molar balances of the compounds (n) and the mass transfer rates are summarized below.

The reaction rates at the surface (r_n), the mass transfer from the liquid phase to the catalyst surface (r_n^{LS}), and from the gas phase to the liquid phase (r_n^{GL}) were described by eqs 2−4, respectively. The indices s, l, and g refer to the solid, liquid, and gaseous phases. The surface reaction rates (r_n) were determined as the product of the surface coverages of reacting components (c_n^s) and reaction constants (k_n), liquid−solid mass transfer coefficient (k_n^l) and solid−liquid interface (A_s), and gas−liquid transfer coefficient (k_n^g) and gas−liquid interface (A_g), while p_n is the partial pressure of a component (n). Further correlations, equations, nomenclature, and units are presented in our previously published works.[23,32−34]

$$r_n = k_n \times c_n^s \tag{2}$$

$$r_n^{SL} = k_n^l \times A_s(c_n^l - c_n^s) \tag{3}$$

$$r_n^{GL} = k_n^g \times A_g \times (p_n/\mathrm{He} - c_n^l) \tag{4}$$

The modeled values for the identified intermediates and products were determined by solving a set of ordinary differential equations describing the molar balances of the relevant components in each phase. The molar balances were considered for the reactant, the intermediates, and the products in the liquid phase (eq 5) and at the catalyst surface (eq 6). Different process conditions (*e.g.*, initial reactant concentration, operating temperature and pressure, catalyst mass, reaction time, and stirring speed), catalyst properties

https://doi.org/10.1021/acscatal.4c06058
ACS Catal. 2025, 15, 1182−1194

(*e.g.*, specific surface area and concentration of active sites), and reactor geometry were considered during kinetic model development.

$$\frac{dC_{n(l)}}{dt} = r_n^{GL} - r_n^{SL} \quad (5)$$

$$\frac{dC_{n(s)}}{dt} = r_n^{SL} \pm \sum r_n \quad (6)$$

Our previous studies[23,32] showed that there are no limitations on internal and external mass transfer for catalyst particles with a size of 50 μm at a stirring speed of 100−1000 rpm. Furthermore, it was assumed that at a heating rate below 7.5 °C min^{-1}, the effects of heat transfer would lead to a negligible temperature gradient within the investigated environment. Consequently, a low heating rate of 5 °C min^{-1} was used to optimize heat transfer and prevent the development of significant temperature gradients. In this study, the combination of intensive mixing and a low heating rate ensured the absence of mass and heat transfer limitations.

The kinetic model was solved using the implicit Runge−Kutta formula to solve the differential equations with Matlab version R2022a software. Nelder−Mead method was used for the regression analysis and optimization of the fitting parameters, k_n and Ea_n, while Levenberg−Marquardt method was then used for the final determination and optimization of 95% confidence intervals based on the Jacobian matrix calculation. The least-squares minimization equation is presented as eq 7 and sums the squared differences between the experimentally ($C_{j,i}^{exp}$) and modeled ($C_{j,i}^{mod}$) determined concentrations for all experiments (EXP), the components (COMP) and the collected samples (SAM), where j is the same experimental condition and i is the time of the sample.[10]

$$f(k_n, Ea_n) = \sum_{j=1}^{EXP} \sum_{i=1}^{SAM} \sum_{C=1}^{COMP} (C_{j,i}^{exp} - C_{j,i}^{mod})^2 \quad (7)$$

5. RESULTS AND DISCUSSION

The lignin model component 2-phenoxy-1-phenylethanol (2P1PE) contains the β-*O*-4 bond, which is the most abundant bond between monolignol units and mimics the most easily cleavable bond in the native lignin structure. To understand the kinetics of its cleavage, DFT calculations and kinetic modeling were performed to determine the bond dissociation energies and kinetic rate parameters, respectively. Furthermore, the conclusions of the cleavage mechanism were upgraded and correlated with the lignin depolymerization study.

5.1. Bond Dissociation Energy. BDEs were calculated for the homolytic bond cleavage since the reaction takes place in a nonpolar environment, and the involved bonds are largely nonpolar. Furthermore, the BDEs for homolytic bond cleavage are less dependent on the solvent or gaseous phase. For simple bond cleavage, it is more likely that the bond with the lowest BDE will be cleaved first. In more complex scenarios, especially when product rearrangements of radical stabilization are possible or interactions with the catalyst change upon cleavage, the trends might differ.

We investigated the BDE of 2-phenoxy-1-phenylethanol (2P1PE, **1**) and phenethoxybenzene (PEB, **2**) and assessed the BDEs of possible different cleavage positions within the binding of dimeric model compounds. The calculated BDEs ranged from 297.9 to 432.2 kJ mol^{-1}, as shown in Table 1. For both compounds, the most likely cleavage point appears to be C_β−O(Ph).

Table 1. Relevant Bond Dissociation Energies, as Calculated at the wB97XD/aug-cc-pVTZ Level, in 2-Phenoxy-1-phenylethanol and Phenethoxybenzene

lignin model compound	Bond	BDE (kJ mol^{-1})
2-Phenoxy-1-phenylethanol (2P1PE, **1**)	R−OH	369.0
2-Phenoxy-1-phenylethanol (2P1PE, **1**)	PhCH(OH)−CH_2OPh	315.5
2-Phenoxy-1-phenylethanol (2P1PE, **1**)	PhCH(OH)CH_2−OPh	302.5
2-Phenoxy-1-phenylethanol (2P1PE, **1**)	PhCH(OH)CH_2O−Ph	430.5
Phenethoxybenzene (PEB, **2**)	$PhCH_2$−CH_2OPh	331.8
Phenethoxybenzene (PEB, **2**)	$PhCH_2CH_2$−OPh	297.9
Phenethoxybenzene (PEB, **2**)	$PhCH_2CH_2$O−Ph	432.2

5.2. Reaction Mechanism and Hydrogenation Results of 2-Phenoxy-1-phenylethanol. The proposed hydrogen-mediated cleavage pathways of 2-phenoxy-1-phenylethanol are shown in Figure 1. The following scenarios are possible. 2P1PE can be dehydrogenated to PEB (Route 1), and cleavage then occurs at the etheric C_β−O or C_{Ar}−O site, yielding aromatic monomers (Route 2 or 4, respectively). Alternatively, in 2P1PE, the alkyl aryl ether bond can be cleaved at the C_β−O or C_{Ar}−O sites (Routes 3 and 5, respectively).

Lu et al.[35] proposed and explained that, 2P1PE is difficult to cleave on Pd catalysts without predehydrogenation (to PEB). Thus, the cleavage reactions in which the C_α−C_β bond and the C_β−O bond are cleaved were excluded as possible initial reactions for 2P1PE degradation. On Pd, they calculated the reaction energy (not BDE!) of C_α−OH bond cleavage as 50 kJ mol^{-1} (converted from the published value of 0.49 eV), while it was 222 kJ mol^{-1} (converted from the published value of 2.30 eV) and 150 kJ mol^{-1} (converted from the published value of 1.55 eV) for C_α−C_β and C_β−O bonds, respectively.[35] Note that these are not BDEs but reaction energies on Pd, which are massively impacted by the stabilization of individual species on the Pd catalyst and are not transferable to gas-phase reactions or other catalysts. On the other hand, Parthasarathi et al.[36] calculated catalyst-independent BDEs for C_β−O and C_α−C_β bonds of 270 kJ mol^{-1} and 315 kJ mol^{-1}, respectively, with the values representing averaged BDEs for different lignin model compounds of β-*O*-4 bonds.

In our study, the DFT calculations of BDE for the C_β−O, C_α−C_β and C_α−OH bonds in the dimeric model compound are 302.5 kJ mol^{-1}, 315.5 kJ mol^{-1}, and 369.0 kJ mol^{-1}, respectively. Based on our experimental results, the dominant reaction mechanism was the dehydroxylation and subsequent hydrogenation of 2P1PE to PEB, as Ni is a known hydrogenation catalyst that readily cleaves OH groups from organic backbones.[37]

The resulting PEB was cleaved by hydrogenolysis to phenol (**PHE**) and ethylbenzene (**EBZ**) (Route 2) or through a less dominant pathway to benzene (**9**) and 2-phenylethanol (**7**) (Route 4). The experimental data showed that Route 2 is more dominant. This was also confirmed by DFT calculations, showing that the BDE of the C_β−O bond (297.9 kJ mol^{-1}) is substantially lower than that of the C_{Ar}−O bond (432.2 kJ mol^{-1}). On the other hand, GC−MS analysis showed that the

https://doi.org/10.1021/acscatal.4c06058
ACS Catal. 2025, 15, 1182−1194

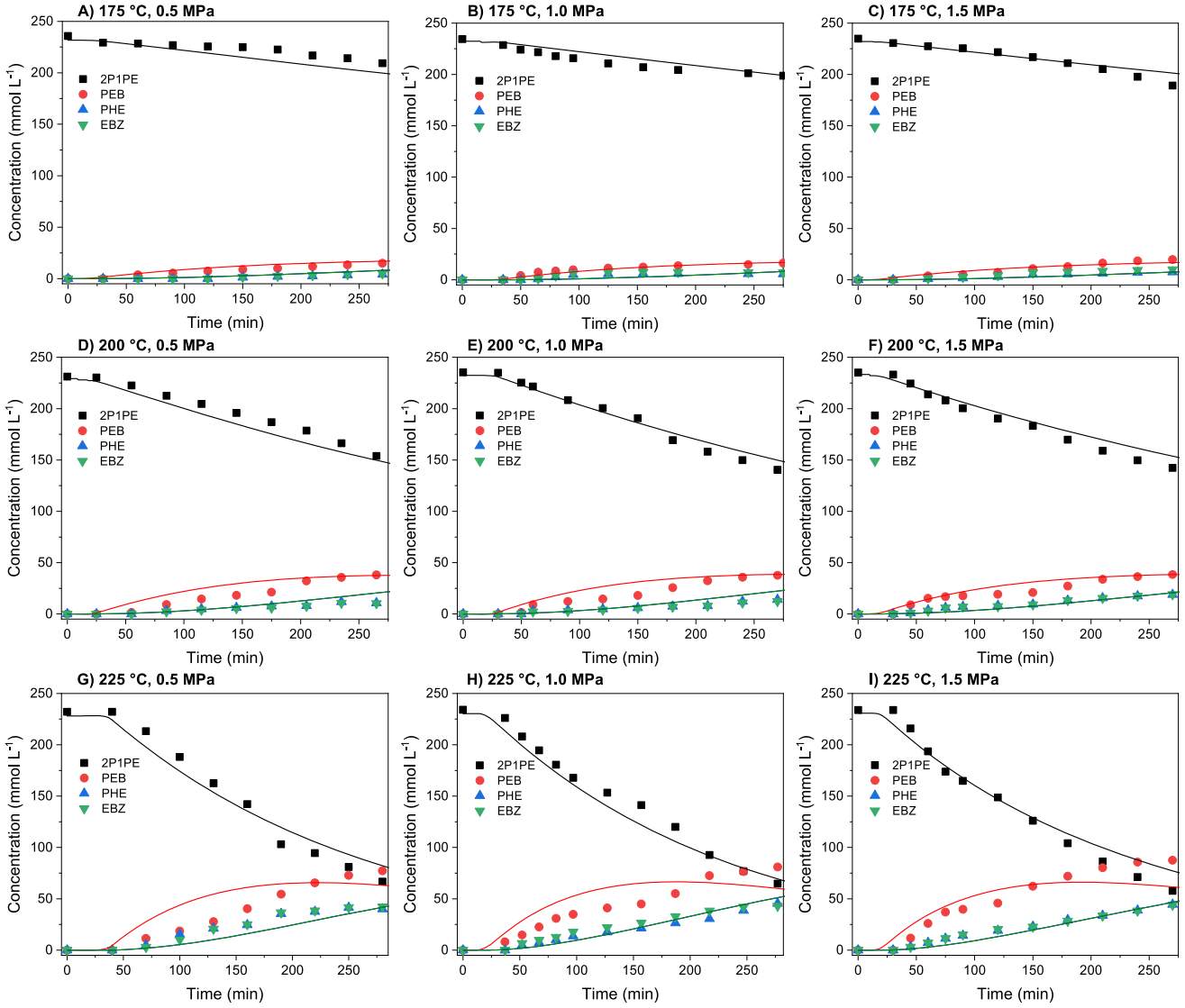

Figure 2. Hydrogenation results of 2P1PE and product distribution of β-*O*-4 bond cleavage over Ni/C catalyst at different temperatures and pressures (points: experimental values; line: modeled values).

products expected from cleavage by the mechanisms proposed by Route 3 and Route 5 were not detected.

The conversion and product distribution of the catalytic cleavage of the β-*O*-4 bond of 2P1PE and PEB are listed in Figure 2. It was found that the reaction temperature had a significant effect on the cleavage of the β-*O*-4 bond in the lignin model compound, whereas higher hydrogen pressure exhibited a less pronounced effect. At a temperature of 175 °C, only a slight predehydrogenation of 2P1PE was observed, the conversion of 2P1PE only reached up to 20%, which is why the yield of monomeric products was only 7.4%. Increasing the temperature to 200 °C and 225 °C sufficiently increased the efficiency of the hydrogenation process. The hydrogenation treatment of 2P1PE at 200 °C resulted in a higher predehydrogenation rate to PEB, while the yield of phenol and ethylbenzene more than doubled to 16.1%. Further increasing the temperature by another 25 °C and analyzing the product distribution revealed that almost 75% of the 2P1PE was prehydrogenated to PEB, which in turn was involved in the cleavage of the β-*O*-4 bond, leading to 37.4 mmol L^{-1} of ethylbenzene and 37.8 mmol L^{-1} of phenol with a yield of 32.1% of total monomers.[38] On the other hand, at higher hydrogen pressure, the intensity of predehydrogenation increased, as less time was needed to obtain the same amount of predehydrogenated dimeric compound (PEB). The product distribution was significantly influenced by the reaction conditions. The Ni/C catalyst showed limited activity in the cleavage of β-*O*-4 bonds within 2-phenoxy-1-phenylethanol and phenethoxybenzene. However, it proved to be effective in maintaining the aromaticity of the resulting monomers and prevented complete ring hydrogenation. To maintain aromaticity, high temperatures, low hydrogen pressure, or an inert atmosphere were found to be essential.[24,35]

Furthermore, the noncatalytic (reference) test was performed at a temperature of 225 °C and a pressure of 1.0 MPa (hydrogen), and it was found that only a minor conversion of 2P1PE of 15% and the removal of the OH group were observed, while no monomers were formed (Figure S1A), suggesting that the use of a Ni/C catalyst was required for the cleavage of the β-*O*-4 bonds within the dimeric lignin compound.

https://doi.org/10.1021/acscatal.4c06058
ACS Catal. 2025, 15, 1182−1194

On the other hand, the effect of ethanol as a hydrogen donor solvent was evaluated by the catalytic test at a temperature of 225 °C and a pressure of 1.0 MPa under inert (nitrogen) atmosphere (Figure S1B). Predehydrogenation and conversion of 2P1PE was approximately 24%, while minor cleavage of the *β-O-4* bond in PEB also occurred, yielding monomeric products of EBZ and PHE of about 4.6% each. Compared with the results obtained after catalytic hydrogenation of 2P1PE, the external hydrogen source increased the monomer yield by 3.5-fold. Therefore, efficient cleavage of the *β-O-4* bond generally requires the presence of an active catalyst and the supply of external hydrogen.

5.3. Kinetic Modeling Results. The reaction rate constants and activation energies (Table 2) for *β-O-4* bond cleavage in 2P1PE were determined by regression analysis using a mathematical kinetic model, while the values of the reactant, intermediates, and products predicted by the model are shown as lines in Figure 2 and compared with the experimental data points. The reaction rate constant for the predehydrogenation of 2P1PE to PEB (k_1) was determined to be 0.35 min^{-1}, while further C_β−O bond cleavage (k_2) occurred at an almost 2-fold higher reaction rate of 0.68 min^{-1}. In Table 2, the activation energy of the predehydrogenation step of 2P1PE to PEB was determined to be 71 kJ mol^{-1}, while we report the activation energy of the cleavage of PEB to PHE and EBZ to be 9 kJ mol^{-1}, indicating that predehydrogenation is a highly important step to decrease the activation energy and increase the reaction rate of *β-O-4* bond cleavage in PEB. In particular, the determined Ea_2 value of 9 ± 9 kJ mol^{-1} showed that this parameter has no effect on the concentration profiles or objective function error when it is lower than 18 kJ mol^{-1}. A low activation energy means that the ether bond cleavage is not significantly affected by temperature (in the investigated temperature range), and the rate depends mainly on the availability of the PEB intermediate concentration. On the other hand, a similar but less drastic trend was suggested by DFT calculations when the BDE for C_β−O bond cleavage decreased from 302.5 kJ mol^{-1} for 2P1PE to 297.9 kJ mol^{-1} for PEB.[38] Furthermore, the kinetic modeling and product distributions of 2P1PE showed that the cleavage of the *β-O-4* bond was not affected by variations in hydrogen pressure within the 0.5 and 1.5 MPa range. This indicated that hydrogen availability in the liquid phase and on the catalyst surface was always sufficient for the cleavage of the *β-O-4* bond; hence, its global rate was not affected by mass transfer limitations but governed by intrinsic reaction kinetics instead.

Table 2. Reaction Rate Constants and Activation Energies for the Cleavage of Lignin Model Compounds

reaction rate constant	min^{-1}	activation energy	kJ mol^{-1}
k_1	0.35 ± 0.04	Ea_1	71 ± 13
k_2	0.68 ± 0.05	Ea_2	9 ± 9

The Ni/C catalyst is particularly effective in reducing the bond dissociation energy to cleave the *β-O-4* bond, while predehydrogenation and removal of the OH group from the organic moiety are crucial steps to facilitate the cleavage at the C_β−O position in PEB.

On the other hand, 2P1PE lacks variations and complexity of lignin structural features, especially the functionality of functional groups *γ*-carbinol, methoxy, and/or hydroxyl group. The bond dissociation energies and the kinetic parameters might be altered due to the additional functionality of the lignin model compounds. Steric hindrances such as *γ*-carbinol, methoxy, and hydroxyl groups influenced the reaction rates, cleavage mechanisms, and reactivity of the *β-O-4* bond.[8,39−41] Sturgeon et al.[40] considered that the *γ*-carbinol group did not affect the reaction rate of *β-O-4* bond cleavage, while it demonstrated that the additional functionality of methoxy and hydroxyl groups led to a 2 orders of magnitude faster reaction rate of *β-O-4* bond cleavage. Catalytic cleavage of *β-O-4* bonds in more complex model compounds could also lead to defunctionalization and removal of methyl, methoxy, or phenolic groups as gaseous products altering the performance and reaction kinetics.[10,41]

Therefore, the additional functionality of lignin model compounds changes the environment of the bonds and functional groups and thus the reactivity of the system.

5.4. Lignin Depolymerization Results. The cleavage of the *β-O-4* bond forms intermediates with different reactivity and stability, which is particularly evident during lignin

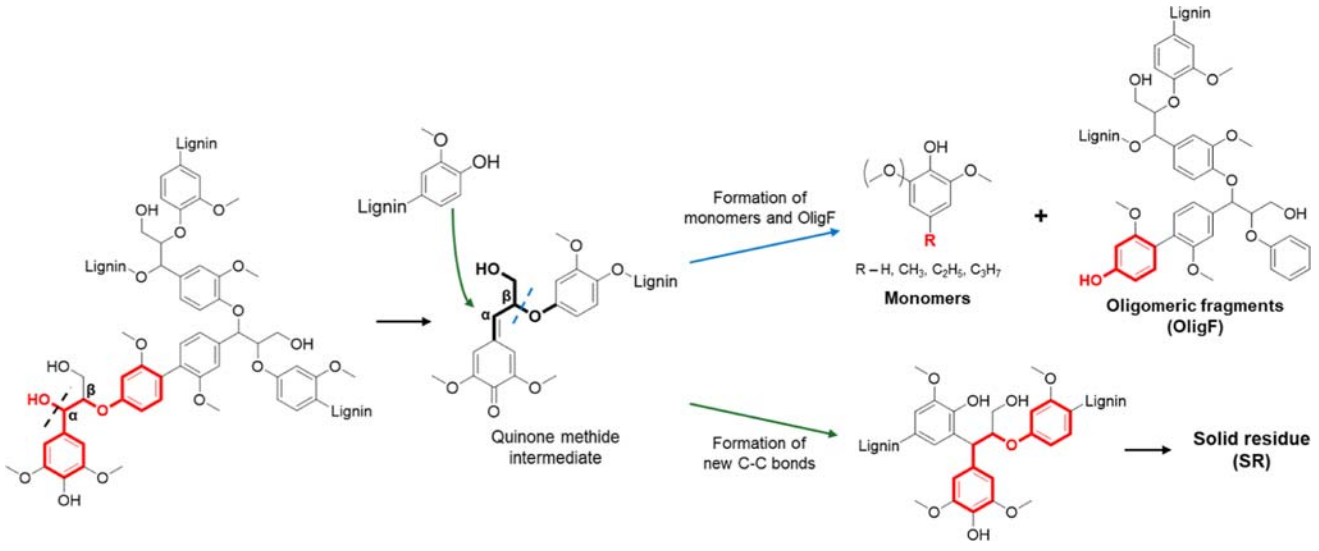

Figure 3. Simplified lignin depolymerization mechanism and cleavage within lignin macromolecule (formation of SR, OligF, and monomers).

https://doi.org/10.1021/acscatal.4c06058
ACS Catal. 2025, 15, 1182−1194

depolymerization. The initial depolymerization mechanism involves the formation of radicals at the C_α-position within the β-*O*-4 lignin units. The cleavage of the β-*O*-4 bond, as well as the removal of OH_α, OH_γ, phenolic OH groups, and other functional groups in lignin, requires the presence of a transition or noble metal catalyst, a hydrogen atmosphere, or/and a hydrogen donating solvent, e.g., ethanol, methanol, or *iso*-propanol.

The study of β-*O*-4 bond cleavage in the hydrogenation of the lignin model compound was extended and linked to lignin depolymerization (LD). The results with the dimeric lignin compound showed that only the variation of the temperatures positively influenced the product distribution. Therefore, similar temperatures with a moderate hydrogen pressure were applied for lignin depolymerization. The streamlined mechanism of lignin depolymerization proceeds through the cleavage of the β-*O*-4 bonds, followed by hydrogenation and stabilization of the reactive radicals formed. The successful cleavage of the β-ether bond and the stabilization of these radicals formed results in smaller oligomeric fragments and phenolic monomers. These phenolic monomers are formed by the cleavage of β-*O*-4 bonds at either lignin inter- or end-units. Li et al.[39] demonstrated that the catalytic cleavage of oligomeric lignin-like model components had similar kinetic parameters for β-*O*-4 bond cleavage at both inter- or end-units. Furthermore, effective cleavage usually occurs through quinone methide or aldehyde intermediates, although the same intermediates may also be involved in coupling reactions. These coupling reactions lead to the formation of C−C bonds and the formation of solid carbon residues, suggesting that the final product distribution depends on the equilibrium between the stabilization of reactive radicals by hydrogenation and the formation of carbon bonds leading to solid residue.[42] The mechanism of coupling within reactive intermediates resulting in recalcitrant products was investigated by Huang et al.[14] and Ročnik Kozmelj et al.,[10] who proposed the formation through the available C_5-position in the neighboring compound, the hydroxyl group, or unsaturated side-chain carbons. Figure 3 shows possible lignin-like structural products and the mechanism of lignin depolymerization described above.

After lignin depolymerization, the products were divided into solid residue (SR), oligomeric fragments (OligF), and monomers based on similar structural characteristics (Figure 4).

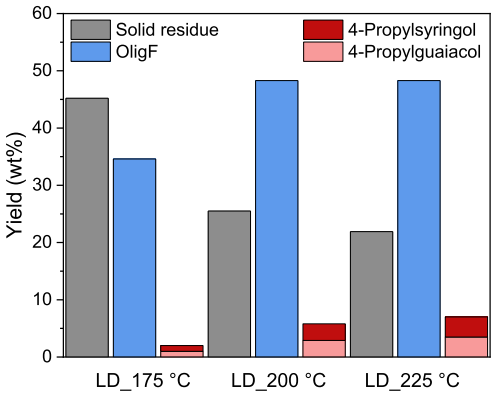

Figure 4. Product distribution of lignin depolymerization at different temperatures and initial set hydrogen pressure of 1.0 MPa.

In catalytic lignin depolymerization, the formation of SR was found to be strongly temperature-dependent, as increasing the temperature from 175 °C to 200 °C drastically reduced the yield of SR from 45.2 wt % to 25.5 wt %. A further increase in temperature by 25 °C led to an additional suppression of SR formation, as the yield of 21.9 wt % was achieved. It is likely that if supercritical conditions are not achieved for ethanol, the hydrogen affinity and H-donor ability of ethanol are less pronounced and less effective in stabilizing reactive radicals at lower temperatures. Therefore, achieving supercritical conditions for ethanol may play a more significant role in preventing coupling reactions,[43] thereby reducing the formation of recalcitrant products.

OligF with a lignin-like aromatic structure is the main product formed during lignin depolymerization, whereby the structural characteristics changed significantly compared to the initial lignin (Table 3). Even at the low temperature of 175 °C, the amount of precipitated OligF was 34.6 wt %. The yield of OligF increased to 48.3 wt % when temperatures of 200 °C and 225 °C were applied. It was found that higher temperatures favored the formation of OligF over SR and are apparently required for the stabilization of the reactive radicals and switching the equilibrium to the formation of OligF instead of SR.

Table 3. Lignin and Oligomeric Fragments: Weight-Average Molecular Weight (M_w), Number-Averaged Molecular Weight (M_n), and Dispersity (Đ)

	Mw (Da)	Mn (Da)	Đ
lignin	3700	1300	2.8
OligF_175	2050	1300	1.6
OligF_200	2100	1200	1.8
OligF_225	1850	1050	1.8

Table 3 and Table 4 show the structural features of lignin and OligF at different temperatures analyzed by SEC, ^{31}P, and 2D-HSQC NMR methods, respectively. The molecular weight distribution (MWD) and NMR spectra are shown in Figure 5 and Figures S3−S10, respectively. By plotting the profiles of MWD of lignin and oligomeric fragments (OligF_temperature in °C) shown in Figure 5, the differences between lignin and depolymerized samples became visible. It was found that the weight-average molecular weight (M_w) of lignin was reduced from 3700 Da to 2050 Da, 2100 Da, and 1850 Da after depolymerization at 175 °C, 200 °C, and 225 °C, respectively (Table 3). Depolymerization of lignin resulted in OligF with a lower M_w, also lowered number-average molecular weight (M_n) and dispersity (Đ). The Mn of lignin was reduced from 1300 Da to 1050 Da of OligF_225, while a lower depolymerization temperature had a minor effect on the M_n. Furthermore, a significant decrease in lignin dispersity from 2.8 to 1.8 was observed, indicating that OligF has a more uniform polymeric structure than lignin.[44]

Analysis of the hydroxyl functional groups by ^{31}P NMR (Table 4) underlined the predehydrogenation of lignin, which was evident in the removal of OH groups at the C_α-position, as the content of aliphatic OH groups decreased from 2.42 mmol g^{-1} to 1.97 mmol g^{-1}, 1.69 mmol g^{-1}, and 1.39 mmol g^{-1} following depolymerization at 175 °C, 200 °C, and 225 °C, respectively. On the other hand, the content of phenolic OH groups increased with depolymerization temperature. For the syringyl OH groups, there was a change from 1.04 mmol g^{-1} in

https://doi.org/10.1021/acscatal.4c06058
ACS Catal. 2025, 15, 1182−1194

Table 4. 2D-HSQC and ^{31}P NMR Results of Lignin and OligF after Lignin Depolymerization

	β-O-4	β-O-4′	β-5	β–β′	ED[a]	Aliph[b]	S[c]	Cond[d]	G[e]	Phen[f]	total
	per 100 C9 units				(%)	OH groups (mmol g^{-1})					
lignin	13.5	12.9	3.3	8.9	49	2.42	1.04	0.65	0.80	2.50	4.96
OligF_175	10.9	13.7	3.2	5.2	56	1.97	1.20	0.81	0.85	2.86	4.88
OligF_200	5.2	8.6	2.1	4.9	60	1.69	1.28	0.89	0.98	3.15	4.93
OligF_225	4.0	9.3	1.9	5.6	70	1.39	1.41	0.96	1.04	3.41	4.83

[a]Ethoxylation degree. [b]Aliphatic OH groups. [c]Syringyl OH groups. [d]Condensed OH groups. [e]Guaiacyl OH groups. [f]Phenolic OH groups.

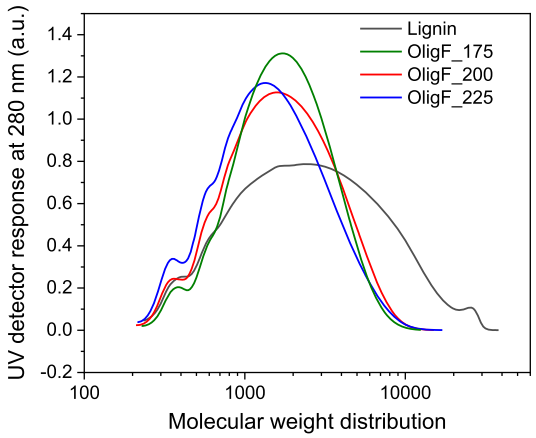

Figure 5. Comparison of molecular weight distributions of lignin and oligomeric fragments after depolymerization at 175 °C, 200 °C, and 225 °C.

lignin to 1.20−1.41 mmol g^{-1} for OligF after LD, while a less remarkable increase from 0.80 mmol g^{-1} in lignin to 0.85−1.04 mmol g^{-1} for OligF was observed for the guaiacyl OH groups. The most significant increase was observed for the condensed OH groups from 0.65 mmol g^{-1} in lignin to 0.96 mmol g^{-1} for OligF after depolymerization at 225 °C.[38] OligF showed a higher content of condensed and C_5-substituted OH groups, suggesting structural rearrangements. The cleavage of the β-ether bond leads primarily to monomers, whereas dimers or larger oligomers contribute to an increased presence of C_5-substituents in the form of β-5 substructures, 5−5′ substructures, and 4-O-5′ substructures through direct C−C coupling of aromatic rings.[45,46] Moreover, Giummarella et al.[47] used advanced NMR characterization of lignin and lignin-like model oligomers to confirm these coupling mechanisms and substructural rearrangements. The changes in hydroxyl group content in OligF strongly indicate that the lignin underwent significant structural changes and intramolecular rearrangements during depolymerization, which is consistent with the observations from previous studies.[42,48] The structural

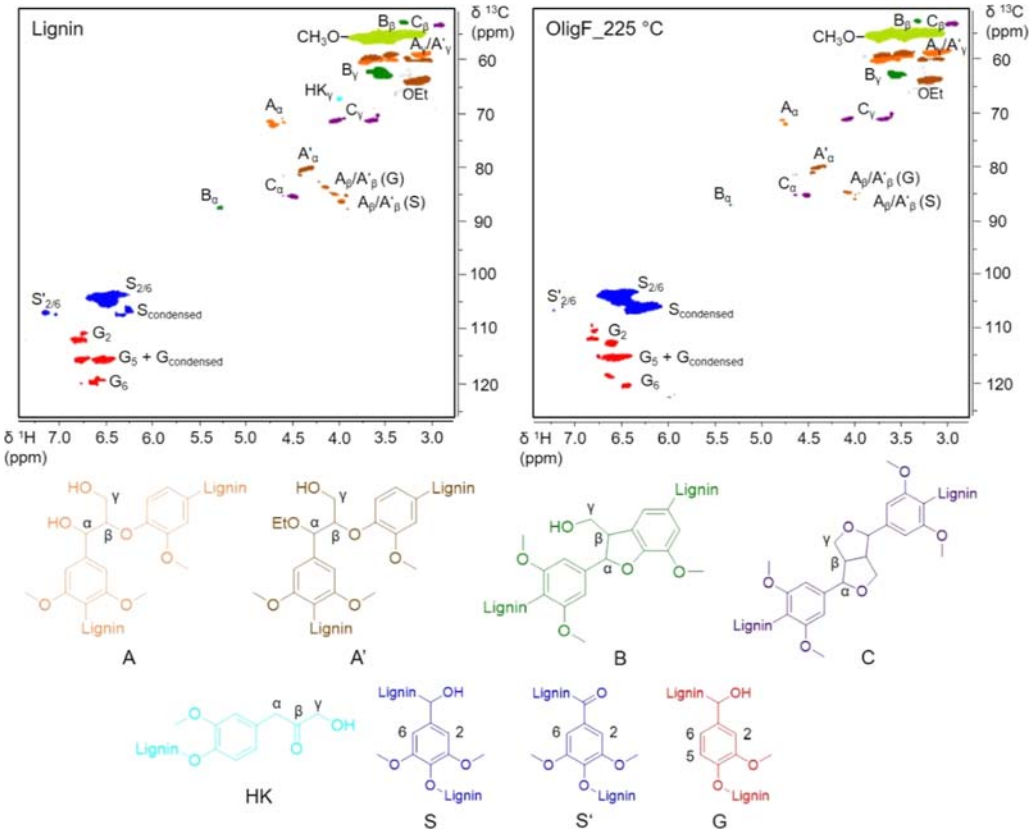

Figure 6. 2D-HSQC spectrum of lignin and oligomeric fragments obtained after lignin depolymerization at 225 °C (OligF_225).

https://doi.org/10.1021/acscatal.4c06058
ACS Catal. 2025, 15, 1182−1194

characteristics of OligF suggest a more condensed structure with a higher content of phenolic OH groups formed by the hydrogenolysis of β-O-4 bonds. Remarkably, the increasing abundance of syringyl OH groups excided that of the guaiacyl OH groups.

The semiquantitative 2D-HSQC method revealed that the β-O-4 and α-ethoxylated β'-O-4 bonds remained present in the OligF samples (Figure 6), indicating that temperatures up to 225 °C are not sufficient for catalytic lignin depolymerization and complete cleavage of the β-ether bonds (Table 4). The ethoxylation degree, defined as the ratio between the β-O-4 and α-ethoxylated β'-O-4 bonds, increased at reaction temperatures of 175 °C, 200 °C, and 225 °C. This indicates that the β-O-4 bonds are more favorably cleaved compared to α-ethoxylated β'-O-4 bonds, likely because these bonds are more sterically hindered by α-ethoxylated aliphatic hydroxyl groups in the C_α-position,[28] which affects the BDE of the bonds and the accessibility of the catalyst to the bonds.[49] On the other hand, an enriched amount of α-ethoxylated β'-O-4 bonds was observed in OligF after depolymerization at 175 °C (13.7 per 100 C9 units) than in the starting lignin (12.9 per 100 C9 units), suggesting that the hydroxyl groups in the C_α-position are ethoxylated rather than removed, favoring alkoxylation reactions similarly as observed in the isolation of ethanol-organosolv lignin.[28,50] Therefore, when lignin was depolymerized at 175 °C, a minor part of β-O-4 bonds was cleaved.

Although no significant depolymerization occurred at 175 °C, the M_w of lignin in OligF decreased from 3700 Da to 2050 Da, and the dispersity was reduced from 2.8 to 1.6. However, the M_n remained unchanged, supporting the theory that no significant depolymerization occurred at this temperature. Smit et al.[48] reported a similar observation in the partial lignin depolymerization of acetone organosolv lignin at 150 °C and ruled out an overestimation of M_w by SEC analysis due to lignin aggregation. The reduction in M_w could instead be due to the removal of impurities such as sugars from cellulose or hemicellulose, which are bound to the lignin structure through weak α-ether bonds and are easily cleavable at temperatures close to or above those of the pulping process.[50,51] Other contributing factors include a low extent of cleavage of β-O-4 bonds,[52] limited recondensation within the structure of OligF due to α-etherified moieties at the C_α-position,[48,50] and limited solubilization of lignin in ethanol.[53] However, the 2D-HSQC results showed that lignin was depolymerized to smaller oligomeric fragments, as even C−C bonds such as β-5 and β−β were slightly less abundant than in the initial lignin.

The liquid samples were analyzed by GC−MS, which revealed the two main monomeric products corresponding to the characteristic monolignol: guaiacyl (G-unit) and syringyl (S-unit) units. The yields of 4-propylguaiacol and 4-propylsyringol increased with an increase in temperature, with 4-propylsyringol being the dominant product. The total monomer yield was between 2.1, 6.6, and 8.0 wt % at depolymerization temperatures of 175 °C, 200 °C, and 225 °C, respectively. These monomer yields correspond to the composition of hardwood lignin, which contains predominantly G- and S-units. The higher yield of 4-propylsyringol, which was about 30% higher than that of 4-propylguaiacol, indicates that syringyl-like units are linked with more easily cleavable β-ether bonds compared to guaiacyl-like units. However, the correlation between the S/G ratio in lignin, the connectivity of the monolignols through β-ether bonds, and the monomer yield after depolymerization was later found to be questionable.[54]

Rinaldi et al.[55] reported that the theoretical yield of lignin-derived monoaromatics from organosolv lignin is between 4 and 35%, depending on the abundance of the cleavable bonds (*e.g.*, β-O-4 bonds) and the number of monomeric units within the lignin macromolecule. For the organosolv lignin used in this study, the calculated theoretical monomer yield[55,56] is approximately 50%, depending on the proportion of the cleavable β-O-4 and α-ethoxylated β'-O-4 bonds (0.68) and the assumed number of monomeric units − n-value (*e.g.*, the n-number for the calculation was 6−8). Detailed equations and calculations can be found in the Supporting Information. The low depolymerization temperature used in this study was not sufficient to achieve maximum theoretical yield, as evidenced by the low monomer yield and the presence of β-O-4 bonds in the precipitated OligF. Nevertheless, achieving the maximum theoretical monomer yield is crucial for promoting cost-effective and efficient biorefinery strategies.[57]

A noncatalytic lignin depolymerization was performed to evaluate the importance of the Ni/C catalyst for the cleavage of the β-O-4 bond and the formation of OligF and monomers at a temperature of 225 °C and a hydrogen pressure of 1.0 MPa. Figure S2A shows the product distribution of non-catalytic treatment, which resulted in 35.7% of SR and 44.1% of OligF, while monomers were not detected. The noncatalytic performance indicated that the rearrangement of lignin was mainly due to the unfavorable formation of C−C bonds and thus SR, while favorable OligF were formed. The presence of ethanol as a hydrogen donor and external hydrogen source therefore only slightly contributed to the stabilization of the reactive intermediates formed without the catalyst. It was beneficial for the formation of OligF, but less effective for the cleavage of the β-O-4 bond to form monomers or to suppress the coupling reactions and the formation of C−C bonds.

Furthermore, the contribution of the hydrogen donor solvent to catalytic lignin depolymerization was evaluated at a temperature of 225 °C and a pressure of 1.0 MPa under an inert (nitrogen) atmosphere. The product distribution showed the formation of SR with a yield of 33.7%, a yield of OligF of 46%, while the yield of monomers was 2.5% (Figure S2B), indicating that only the hydrogen donor solvent has a minor contribution to the formation of monomeric products. Similarly to the dimeric model compound, the efficient lignin depolymerization requires the presence of the Ni/C catalyst and the supply of external hydrogen.

We reported a mass balance of about 80% for the product distribution. The remaining mass is probably due to the losses during the experimental procedure, measurement, and calculation errors for monomeric products and assumptions regarding the formation of gaseous byproducts, such as H_2O, CO, CO_2, and CH_4 during lignin hydrotreating, which mainly result from defunctionalisation.[42,58] Moreover, smaller lignin fragments (e.g., dimers, trimers, etc.) could remain undetected due to the detection limits of the GC−MS analysis or remain soluble in the liquid after precipitation of oligomeric fragments.[54]

5.5. Process- and Structure-Dependent Correlations between the Lignin Model Compound and Lignin. Lignin model compounds have been used extensively to gain a fundamental and mechanistic understanding of the behavior of lignin in various processes and to correlate the research with the lignin macromolecule.[10,20,59,60] This approach has provided

https://doi.org/10.1021/acscatal.4c06058
ACS Catal. 2025, 15, 1182−1194

valuable insights into the reactivity and chemistry of lignin in a more controlled and manageable environment. While the use of lignin model compounds simplifies the complex reactant and product distribution, reaction mechanism, and identification of motifs in lignin, there are also significant limitations, which must be considered. Research using lignin model compounds often lacks the structural variability and complexity of native lignin, and the 3D structure of lignin can rarely be mimicked. Furthermore, the product streams and downstream technologies in such studies may not accurately reflect conditions in real lignin systems. Lahive et al.[8] have critically pointed out that hydrotreatment processes that work well in less complex environments may fail or lead to catalyst deactivation when applied to real lignin samples. It is therefore important and advisable to extend studies using lignin model components with real lignin in the same system.

Lignin depolymerization was applied after studies with lignin model compounds lacking the process- and structure-dependent correlations with further discussion on how studies with lignin model compounds contributed to the understanding and design of lignin depolymerization. Therefore, we proposed and critically evaluated the correlations and predictions for a beneficial combined study with lignin and model compounds.

5.5.1. Process-Dependent Correlations. The *β-O*-4 bond is the most abundant bond in the native lignin structure, and as such, the simplest representation of this unit was used in this study to simulate its cleavage during lignin depolymerization. The first step of *β-O*-4 cleavage in the lignin model compound 2P1PE involved predehydrogenation and removal of the OH group in the C_α-position, which proceeded similarly to lignin depolymerization, as shown by the reduced content of the aliphatic OH groups. However, no significant decrease in the abundance of *β-O*-4 bonds, as determined by 2D-HSQC, was observed at 175 °C. Therefore, the hydrotreatment of both the lignin model compound and the lignin was not very efficient at a temperature of 175 °C, as *β-O*-4 units remained present in both cases. Increasing the temperature to 225 °C resulted in an almost 80% predehydrogenation of 2P1PE to PEB, yielding about 35% monomeric products. In contrast, the organosolv lignin was not completely depolymerized with about 50% of the *β-O*-4 units still present in the OligF samples under the same reaction conditions. However, the monomer yield obtained from lignin was 8%, which is a reasonable yield given the large structural diversity of the starting materials and is a suitable approximation of the supplementary operating conditions.

The lignin model compound provided a reasonable prediction of *β-O*-4 bond cleavage during lignin depolymerization, suggesting that the use of such a model is beneficial for testing catalyst activity in simpler systems. In addition, similarities in the process mechanism were found for both the lignin model compound and lignin, particularly in predehydrogenation of the OH groups. This indicated that the mechanism probably proceeds through similar reactive sites and intermediates. However, the use of 2P1PE as a lignin model compound did not allow the prediction of side reactions or the formation of solid residue during lignin depolymerization.

To further investigate the process-dependent correlations, the turnover frequency (TOF) for the lignin model compound and lignin was calculated and compared to evaluate the catalyst activity for the generation of monomeric products and cleavage of the *β-O*-4 bond (Table 5). TOF was defined by the correspondence of the monomers produced, the number of active sites of the Ni/C catalyst, and the reaction time.[61] Figure S11 clearly demonstrates that the TOF correlates with temperature for lignin and the lignin model compound, i.e., the hydrogenation and depolymerization, respectively. It is noteworthy that 2P1PE shows a more favorable response and exhibits higher efficiency and productivity with increasing temperature for 50 °C compared to lignin. The linear coefficient for the lignin model compound was $4.7 \times 10^{\circ}$, while for lignin, it was 3.9×10^{-2}, indicating that the increased temperature has a significantly greater effect on the cleavage of *β-O*-4 bonds in the lignin model compound, by a factor of almost 120 compared to lignin. This temperature-induced trend enhances the catalytic process and is therefore particularly favorable in a less complex system. This result is significant, as it indicates that the cleavage of the *β-O*-4 bonds occurs at higher reaction rates in the lignin model compound than in lignin. Understanding this difference is crucial, especially when applying kinetic modeling of lignin depolymerization, as the reaction rates determined for lignin model compounds may not be fully transferable to real lignin samples. In addition, the structural diversity of the two reactants plays a key role in the observed variations of the determined parameters.

Table 5. Turnover Frequency of the Lignin Model Compound and Lignin

temperature[a]	TOF lignin model compound (h^{-1})	TOF lignin (h^{-1})
175	73.0	0.84
200	191.7	2.62
225	309.1	2.80

[a]At pressure of 1 MPa.

The process temperature plays a decisive role in controlling the efficiency of lignin (model compound) depolymerization. A temperature of 225 °C is considered the absolute minimum for effective cleavage of the *β-O*-4 bonds in lignin in the presence of a Ni/C catalyst, ethanol, and hydrogen. However, while the lignin model compound provides a good approximation for evaluating catalyst activity, turnover frequency, and potential for catalytic hydrotreating reactions, the yield of lignin monomers and the formation of solid residue are difficult to predict based on studies with the model compound.

5.5.2. Structure-Dependent Correlations. A simple lignin model compound represents the simplest structure of a linkage between the units in lignin, which makes it difficult to establish structural correlations between them. While studies with the lignin model compounds often lead to the formation of two monomers under different conditions and yields, lignin depolymerization follows a more complex reaction pathway. In addition, the structure of the resulting products is also not fully defined and specified. The structural characteristics of lignin or OligF products are dependent on the reaction conditions, which significantly affected the functionality and molecular weight distribution. Thus, predicting the product distribution, functionality, and molecular weight distribution of oligomeric fragments resulting from lignin depolymerization can be difficult and limited based on studying the lignin model compound.

https://doi.org/10.1021/acscatal.4c06058
ACS Catal. 2025, 15, 1182−1194

6. CONCLUSIONS

In this study, the cleavage of the β-ether bond was investigated in a lignin model compound as well as in lignin, focusing on the determination of the kinetic parameters. The Ni/C catalyst proved to be effective in the hydrogenation of the two reactants at the highest tested temperature of 225 °C, with lignin depolymerization of up to 50% being achieved. The reaction pathway showed that the predehydrogenation of 2-phenoxy-1-phenylethanol occurred prior to the cleavage of the β-O-4 bond, similarly evident by a 45% decrease in the content of aliphatic OH groups during lignin depolymerization. The development of the kinetic model confirmed the suitability of the lignin model compound with β-O-4 bond as a starting compound and enabled the establishment of an advanced and highly predictive model that serves as the basis for the kinetic modeling of lignin depolymerization. However, the kinetic model for lignin depolymerization goes beyond the state-of-the-art of this study, thus process- and structure-dependent correlations were proposed. The results highlighted a temperature dependence of β-O-4 bond cleavage, which was required for effective hydrogenation of the lignin model compound and lignin depolymerization. The comprehensive mechanism of lignin depolymerization remains scarcely defined as it is difficult to predict the positions of the cleavage and side reactions, although the comparative study suggested that aliphatic OH groups were removed and further cleavage of the β-O-4 bond occurred at the C_β−O position. The product distribution of lignin depolymerization and the structural characteristics of the oligomeric fragments, in particular the molecular weight and functionality, were affected and process-dependent by temperature, whereby the functionality and reactivity of the oligomers cannot be clearly foreseen by studying the dimeric model compound. The investigation of lignin depolymerization using a model component without mapping and applying the optimal reaction conditions of the model system to a real lignin sample therefore provides an incomplete understanding of the process.

Nevertheless, we believe that modeling the kinetics of a real lignin sample is challenging and requires significant mathematical knowledge to develop high-quality predictive models for biorefineries. Therefore, future work will likely include and require additional lignin-like intermediate molecules, e.g., oligomers, fractionated oligomers, or lignin, to bridge the knowledge gap between the easily predicted systems and the complex (bio)polymer molecules.

■ ASSOCIATED CONTENT

Supporting Information

The Supporting Information is available free of charge at https://pubs.acs.org/doi/10.1021/acscatal.4c06058.

Hydrogenation and depolymerization results of non-catalytic test and catalytic test under inert atmosphere, ^{31}P NMR and 2D HSQC NMR spectra, calculation of theoretical monomer yield, and turnover frequency (PDF)

■ AUTHOR INFORMATION

Corresponding Authors

Edita Jasiukaitytė-Grojzdek − *Department of Catalysis and Chemical Reaction Engineering, National Institute of Chemistry, Ljubljana 1001, Slovenia;* orcid.org/0000-0001-9065-5761; Email: edita.jasiukaitytе@ki.si

Miha Grilc − *Department of Catalysis and Chemical Reaction Engineering, National Institute of Chemistry, Ljubljana 1001, Slovenia; University of Nova Gorica, Nova Gorica 5000, Slovenia;* orcid.org/0000-0002-8255-647X; Email: miha.grilc@ki.si

Authors

Tina Ročnik Kozmelj − *Department of Catalysis and Chemical Reaction Engineering, National Institute of Chemistry, Ljubljana 1001, Slovenia; University of Nova Gorica, Nova Gorica 5000, Slovenia*

Matej Huš − *Department of Catalysis and Chemical Reaction Engineering, National Institute of Chemistry, Ljubljana 1001, Slovenia; Association for Technical Culture of Slovenia (ZOTKS), Ljubljana 1000, Slovenia; Institute for the Protection of Cultural Heritage of Slovenia (ZVKDS), Ljubljana 1000, Slovenia;* orcid.org/0000-0002-8318-5121

Blaž Likozar − *Department of Catalysis and Chemical Reaction Engineering, National Institute of Chemistry, Ljubljana 1001, Slovenia;* orcid.org/0000-0001-7226-4302

Complete contact information is available at: https://pubs.acs.org/10.1021/acscatal.4c06058

Notes

The authors declare no competing financial interest.

■ ACKNOWLEDGMENTS

This work was supported by the Slovenian Research Agency: research core funding P2-0152 (B.L.), research projects N2-0242 (M.G.), J1-3020 (M.H.), J7-4638 (B.L.), N2-0316 (T.R.K.), and L2-50050 (E.J.G.) and infrastructure funding I0-0039 (M.H.). The authors gratefully acknowledge the HPC RIVR consortium and EuroHPC JU for funding this research by providing computing resources of the HPC system Vega at the Institute of Information Science in Maribor, Slovenia.

■ REFERENCES

(1) Sethupathy, S.; Murillo Morales, G.; Gao, L.; Wang, H.; Yang, B.; Jiang, J.; Sun, J.; Zhu, D. Lignin Valorization: Status, Challenges and Opportunities. *Bioresour. Technol.* **2022**, *347*, 126696.

(2) Deng, W.; Feng, Y.; Fu, J.; Guo, H.; Guo, Y.; Han, B.; Jiang, Z.; Kong, L.; Li, C.; Liu, H.; Nguyen, P. T. T.; Ren, P.; Wang, F.; Wang, S.; Wang, Y.; Wang, Y.; Wong, S. S.; Yan, K.; Yan, N.; Yang, X.; Zhang, Y.; Zhang, Z.; Zeng, X.; Zhou, H. Catalytic Conversion of Lignocellulosic Biomass into Chemicals and Fuels. *Green Energy Environ.* **2023**, *8* (1), 10−114.

(3) Sharma, V.; Tsai, M.-L.; Nargotra, P.; Chen, C.-W.; Sun, P.-P.; Singhania, R. R.; Patel, A. K.; Dong, C.-D. Journey of Lignin from a Roadblock to Bridge for Lignocellulose Biorefineries: A Comprehensive Review. *Sci. Total Environ.* **2023**, *861*, 160560.

(4) Ročnik, T.; Likozar, B.; Jasiukaitytė-Grojzdek, E.; Grilc, M. Catalytic Lignin Valorisation by Depolymerisation, Hydrogenation, Demethylation and Hydrodeoxygenation: Mechanism, Chemical Reaction Kinetics and Transport Phenomena. *Chem. Eng. J.* **2022**, *448* (May), 137309.

(5) Ciesielski, P. N.; Pecha, M. B.; Lattanzi, A. M.; Bharadwaj, V. S.; Crowley, M. F.; Bu, L.; Vermaas, J. V.; Steirer, K. X.; Crowley, M. F. Advances in Multiscale Modeling of Lignocellulosic Biomass. *ACS Sustain. Chem. Eng.* **2020**, *8* (9), 3512−3531.

(6) Forchheim, D.; Hornung, U.; Kruse, A.; Sutter, T. Kinetic Modelling of Hydrothermal Lignin Depolymerisation. *Waste Biomass Valorization* **2014**, *5* (6), 985−994.

(7) Obeid, R.; Smith, N.; Lewis, D. M.; Hall, T.; van Eyk, P. A Kinetic Model for the Hydrothermal Liquefaction of Microalgae, Sewage Sludge and Pine Wood with Product Characterisation of Renewable Crude. *Chem. Eng. J.* **2022**, *428* (April 2021), 131228.
(8) Lahive, C. W.; Kamer, P. C. J.; Lancefield, C. S.; Deuss, P. J. An Introduction to Model Compounds of Lignin Linking Motifs; Synthesis and Selection Considerations for Reactivity Studies. *ChemSusChem* **2020**, *13* (17), 4238−4265.
(9) Bjelić, A.; Likozar, B.; Grilc, M. Scaling of Lignin Monomer Hydrogenation, Hydrodeoxygenation and Hydrocracking Reaction Micro-Kinetics over Solid Metal/Acid Catalysts to Aromatic Oligomers. *Chem. Eng. J.* **2020**, *399* (March), 125712.
(10) Ročnik Kozmelj, T.; Žula, M.; Teržan, J.; Likozar, B.; Maver, U.; Činč Ćurić, L.; Jasiukaitytė-Grojzdek, E.; Grilc, M. Understanding Stability, Oligomerization and Deactivation during Catalytic Lignin Hydrodeoxygenation by Mechanistic Reaction Micro-Kinetics Linked with 3D Catalyst Particle Nanotomography. *J. Clean. Prod.* **2023**, *414* (April), 137701.
(11) Schutyser, W.; Renders, T.; Van Den Bosch, S.; Koelewijn, S. F.; Beckham, G. T.; Sels, B. F. Chemicals from Lignin: An Interplay of Lignocellulose Fractionation, Depolymerisation, and Upgrading. *Chem. Soc. Rev.* **2018**, *47* (3), 852−908.
(12) Wang, Y.; Wei, L.; Hou, Q.; Mo, Z.; Liu, X.; Li, W. A Review on Catalytic Depolymerization of Lignin towards High-Value Chemicals: Solvent and Catalyst. *Fermentation* **2023**, *9* (4), 386.
(13) Besse, X.; Schuurman, Y.; Guilhaume, N. Reactivity of Lignin Model Compounds through Hydrogen Transfer Catalysis in Ethanol/Water Mixtures. *Appl. Catal., B* **2017**, *209*, 265−272.
(14) Huang, X.; Korányi, T. I.; Boot, M. D.; Hensen, E. J. M. Catalytic Depolymerization of Lignin in Supercritical Ethanol. *ChemSusChem* **2014**, *7* (8), 2276−2288.
(15) Shen, Z.; Shi, C.; Liu, F.; Wang, W.; Ai, M.; Huang, Z.; Zhang, X.; Pan, L.; Zou, J. Advances in Heterogeneous Catalysts for Lignin Hydrogenolysis. *Adv. Sci.* **2024**, *11* (1), No. e2306693.
(16) Chio, C.; Sain, M.; Qin, W. Lignin Utilization: A Review of Lignin Depolymerization from Various Aspects. *Renew. Sustain. Energy Rev.* **2019**, *107* (February), 232−249.
(17) Xu, J.; Li, C.; Dai, L.; Xu, C.; Zhong, Y.; Yu, F.; Si, C. Biomass Fractionation and Lignin Fractionation towards Lignin Valorization. *ChemSusChem* **2020**, *13* (17), 4284−4295.
(18) Lancefield, C. S.; Panovic, I.; Deuss, P. J.; Barta, K.; Westwood, N. J. Pre-Treatment of Lignocellulosic Feedstocks Using Biorenewable Alcohols: Towards Complete Biomass Valorisation. *Green Chem.* **2017**, *19* (1), 202−214.
(19) Gómez-Monedero, B.; Ruiz, M. P.; Bimbela, F.; Faria, J. Selective Hydrogenolysis of α O 4, β O 4, 4 O 5 C O Bonds of Lignin-Model Compounds and Lignin-Containing Stillage Derived from Cellulosic Bioethanol Processing. *Appl. Catal. A Gen.* **2017**, *541*, 60−76.
(20) Jiang, L.; Xu, G.; Fu, Y. Catalytic Cleavage of the C−O Bond in Lignin and Lignin-Derived Aryl Ethers over Ni/AlP y O x Catalysts. *ACS Catal.* **2022**, *12* (15), 9473−9485.
(21) Li, H.; Liu, M.; Zou, W.; Lv, Y.; Liu, Y.; Chen, L. Selective Hydrodeoxygenation of Lignin and Its Derivatives without Initial Reaction Pressure Using MOF-Derived Carbon-Supported Nickel Composites. *ACS Sustain. Chem. Eng.* **2022**, *10* (17), 5430−5440.
(22) Zhang, J.; Teo, J.; Chen, X.; Asakura, H.; Tanaka, T.; Teramura, K.; Yan, N. A Series of NiM (M = Ru, Rh, and Pd) Bimetallic Catalysts for Effective Lignin Hydrogenolysis in Water. *ACS Catal.* **2014**, *4* (5), 1574−1583.
(23) Bjelić, A.; Grilc, M.; Huš, M.; Likozar, B. Hydrogenation and Hydrodeoxygenation of Aromatic Lignin Monomers over Cu/C, Ni/C, Pd/C, Pt/C, Rh/C and Ru/C Catalysts: Mechanisms, Reaction Micro-Kinetic Modelling and Quantitative Structure-Activity Relationships. *Chem. Eng. J.* **2019**, *359*, 305−320.
(24) Shivhare, A.; Jampaiah, D.; Bhargava, S. K.; Lee, A. F.; Srivastava, R.; Wilson, K. Hydrogenolysis of Lignin-Derived Aromatic Ethers over Heterogeneous Catalysts. *ACS Sustain. Chem. Eng.* **2021**, *9* (9), 3379−3407.
(25) Šivec, R.; Huš, M.; Likozar, B.; Grilc, M. Furfural Hydrogenation over Cu, Ni, Pd, Pt, Re, Rh and Ru Catalysts: Ab Initio Modelling of Adsorption, Desorption and Reaction Micro-Kinetics. *Chem. Eng. J.* **2022**, *436*, 135070.
(26) Jasiukaitytė-Grojzdek, E.; Huš, M.; Grilc, M.; Likozar, B. Acid-Catalyzed α-O-4 Aryl-Ether Cleavage Mechanisms in (Aqueous) γ-Valerolactone: Catalytic Depolymerization Reactions of Lignin Model Compound during Organosolv Pretreatment. *ACS Sustain. Chem. Eng.* **2020**, *8* (47), 17475−17486.
(27) Tran, F.; Lancefield, C. S.; Kamer, P. C. J.; Lebl, T.; Westwood, N. J. Selective Modification of the β−β Linkage in DDQ-Treated Kraft Lignin Analysed by 2D NMR Spectroscopy. *Green Chem.* **2015**, *17* (1), 244−249.
(28) Zijlstra, D. S.; De Santi, A.; Oldenburger, B.; De Vries, J.; Barta, K.; Deuss, P. J. Extraction of Lignin with High β-O-4 Content by Mild Ethanol Extraction and Its Effect on the Depolymerization Yield. *J. Vis. Exp.* **2019**, No. 143, No. e58575.
(29) Meng, X.; Crestini, C.; Ben, H.; Hao, N.; Pu, Y.; Ragauskas, A. J.; Argyropoulos, D. S. Determination of Hydroxyl Groups in Biorefinery Resources via Quantitative 31P NMR Spectroscopy. *Nat. Protoc.* **2019**, *14* (9), 2627−2647.
(30) Chai, J.-D.; Head-Gordon, M. Long-Range Corrected Hybrid Density Functionals with Damped Atom−Atom Dispersion Corrections. *Phys. Chem. Chem. Phys.* **2008**, *10* (44), 6615.
(31) Kendall, R. A.; Dunning, T. H.; Harrison, R. J. Electron Affinities of the First-Row Atoms Revisited. Systematic Basis Sets and Wave Functions. *J. Chem. Phys.* **1992**, *96*, 6796−6806.
(32) Bjelić, A.; Grilc, M.; Likozar, B. Catalytic Hydrogenation and Hydrodeoxygenation of Lignin-Derived Model Compound Eugenol over Ru/C: Intrinsic Microkinetics and Transport Phenomena. *Chem. Eng. J.* **2018**, *333* (September 2017), 240−259.
(33) Hočevar, B.; Grilc, M.; Huš, M.; Likozar, B. Mechanism Ab Initio Calculations and Microkinetics of Hydrogenation, Hydrodeoxygenation, Double Bond Migration and Cis−Trans Isomerisation during Hydrotreatment of C6 Secondary Alcohol Species and Ketones. *Appl. Catal., B* **2017**, *218*, 147−162.
(34) Bjelić, A.; Grilc, M.; Likozar, B. Bifunctional Metallic-Acidic Mechanisms of Hydrodeoxygenation of Eugenol as Lignin Model Compound over Supported Cu, Ni, Pd, Pt, Rh and Ru Catalyst Materials. *Chem. Eng. J.* **2020**, *394* (July 2019), 124914.
(35) Lu, J.; Wang, M.; Zhang, X.; Heyden, A.; Wang, F. β-O-4 Bond Cleavage Mechanism for Lignin Model Compounds over Pd Catalysts Identified by Combination of First-Principles Calculations and Experiments. *ACS Catal.* **2016**, *6* (8), 5589−5598.
(36) Parthasarathi, R.; Romero, R. A.; Redondo, A.; Gnanakaran, S. Theoretical Study of the Remarkably Diverse Linkages in Lignin. *J. Phys. Chem. Lett.* **2011**, *2* (20), 2660−2666.
(37) Fang, Z.; Fan, H.; Zhao, X.; Lin, G.; Li, B.; Wang, J.; Lu, X.; Yang, W.; Li, M.; Song, W.; Fu, J. Unveiling the Nature of Glucose Hydrogenation over Raney Ni: DFT and AIMD Simulations. *Appl. Catal. A Gen.* **2023**, *667*, 119462.
(38) Ročnik, T. Reaction mechanism and microkinetics of heterogeneously catalysed lignin depolymerisation and (de)-functionalization. Ph.D. Dissertation; University of Nova Gorica, Nova Gorica, 2024; . https://repozitorij.ung.si/IzpisGradiva.php?id=9414&lang=eng.
(39) Li, Y.; Demir, B.; Vázquez Ramos, L. M.; Chen, M.; Dumesic, J. A.; Ralph, J. Kinetic and Mechanistic Insights into Hydrogenolysis of Lignin to Monomers in a Continuous Flow Reactor. *Green Chem.* **2019**, *21* (13), 3561−3572.
(40) Sturgeon, M. R.; Kim, S.; Lawrence, K.; Paton, R. S.; Chmely, S. C.; Nimlos, M.; Foust, T. D.; Beckham, G. T. A Mechanistic Investigation of Acid-Catalyzed Cleavage of Aryl-Ether Linkages: Implications for Lignin Depolymerization in Acidic Environments. *ACS Sustain. Chem. Eng.* **2014**, *2* (3), 472−485.
(41) Harth, F. M.; Hočevar, B.; Kozmelj, T. R.; Jasiukaitytė-Grojzdek, E.; Blüm, J.; Fiedel, M.; Likozar, B.; Grilc, M. Selective Demethylation Reactions of Biomass-Derived Aromatic Ether

https://doi.org/10.1021/acscatal.4c06058
ACS Catal. 2025, 15, 1182−1194

Polymers for Bio-Based Lignin Chemicals. *Green Chem.* **2023**, *25*, 10117.
(42) Kozmelj, T. R.; Bartolomei, E.; Dufour, A.; Leclerc, S.; Arnoux, P.; Likozar, B.; Jasiukaitytė-Grojzdek, E.; Grilc, M.; Le Brech, Y. Oligomeric Fragments Distribution, Structure and Functionalities upon Ruthenium-Catalyzed Technical Lignin Depolymerization. *Biomass Bioenergy* **2024**, *181* (December 2023), 107056.
(43) Huang, X.; Korányi, T. I.; Boot, M. D.; Hensen, E. J. M. Ethanol as Capping Agent and Formaldehyde Scavenger for Efficient Depolymerization of Lignin to Aromatics. *Green Chem.* **2015**, *17* (11), 4941−4950.
(44) Jasiukaitytė, E.; Kunaver, M.; Crestini, C. Lignin Behaviour during Wood Liquefaction Lignin Behaviour during Wood Liquefaction - Characterization by Quantitative 31P, 13C NMR and Size-Exclusion Chromatography−Characterization by Quantitative 31P, 13C NMR and Size-Exclusion Chromatography. *Catal. Today* **2010**, *156* (1−2), 23−30.
(45) Gierer, J. Chemical Aspects of Kraft Pulping. *Wood Sci. Technol.* **1980**, *14* (4), 241−266.
(46) Granata, A.; Argyropoulos, D. S. 2-Chloro-4,4,5,5-Tetramethyl-1,3,2-Dioxaphospholane a Reagent for the Accurate Determination of the Uncondensed and Condensed Phenolic Moieties in Lignins. *J. Agric. Food Chem.* **1995**, *43* (6), 1538−1544.
(47) Giummarella, N.; Lindén, P. A.; Areskogh, D.; Lawoko, M. Fractional Profiling of Kraft Lignin Structure: Unravelling Insights on Lignin Reaction Mechanisms. *ACS Sustain. Chem. Eng.* **2020**, *8* (2), 1112−1120.
(48) Smit, A. T.; Dezaire, T.; Riddell, L. A.; Bruijnincx, P. C. A. Reductive Partial Depolymerization of Acetone Organosolv Lignin to Tailor Lignin Molar Mass, Dispersity, and Reactivity for Polymer Applications. *ACS Sustain. Chem. Eng.* **2023**, *11* (15), 6070−6080.
(49) Zhang, C.; Shen, X.; Jin, Y.; Cheng, J.; Cai, C.; Wang, F. Catalytic Strategies and Mechanism Analysis Orbiting the Center of Critical Intermediates in Lignin Depolymerization. *Chem. Rev.* **2023**, *123* (8), 4510−4601.
(50) Jasiukaitytė-Grojzdek, E.; Huš, M.; Grilc, M.; Likozar, B. Acid-Catalysed α-O-4 Aryl-Ether Bond Cleavage in Methanol/(Aqueous) Ethanol: Understanding Depolymerisation of a Lignin Model Compound during Organosolv Pretreatment. *Sci. Rep.* **2020**, *10* (1), 11037.
(51) Nishimura, H.; Kamiya, A.; Nagata, T.; Katahira, M.; Watanabe, T. Direct Evidence for α Ether Linkage between Lignin and Carbohydrates in Wood Cell Walls. *Sci. Rep.* **2018**, *8* (1), 6538.
(52) Gao, F.; Webb, J. D.; Sorek, H.; Wemmer, D. E.; Hartwig, J. F. Fragmentation of Lignin Samples with Commercial Pd/C under Ambient Pressure of Hydrogen. *ACS Catal.* **2016**, *6*, 7385−7392.
(53) Goldmann, W. M.; Ahola, J.; Mikola, M.; Tanskanen, J. Solubility and Fractionation of Indulin AT Kraft Lignin in Ethanol-Water Media. *Sep. Purif. Technol.* **2019**, *209* (June 2018), 826−832.
(54) Anderson, E. M.; Stone, M. L.; Katahira, R.; Reed, M.; Muchero, W.; Ramirez, K. J.; Beckham, G. T.; Román-Leshkov, Y. Differences in S/G Ratio in Natural Poplar Variants Do Not Predict Catalytic Depolymerization Monomer Yields. *Nat. Commun.* **2019**, *10* (1), 2033.
(55) Rinaldi, R.; Jastrzebski, R.; Clough, M. T.; Ralph, J.; Kennema, M.; Bruijnincx, P. C. A.; Weckhuysen, B. M. Paving the Way for Lignin Valorisation: Recent Advances in Bioengineering, Biorefining and Catalysis. *Angew. Chem., Int. Ed.* **2016**, *55* (29), 8164−8215.
(56) Wang, S.; Li, W. X.; Yang, Y. Q.; Chen, X.; Ma, J.; Chen, C.; Xiao, L. P.; Sun, R. C. Unlocking Structure−Reactivity Relationships for Catalytic Hydrogenolysis of Lignin into Phenolic Monomers. *ChemSusChem* **2020**, *13* (17), 4548−4556.
(57) Tofani, G.; Jasiukaitytė-Grojzdek, E.; Grilc, M.; Likozar, B. Organosolv Biorefinery: Resource-Based Process Optimisation, Pilot Technology Scale-up and Economics. *Green Chem.* **2024**, *26* (1), 186−201.
(58) Luo, L.; Yang, J.; Yao, G.; Jin, F. Controlling the Selectivity to Chemicals from Catalytic Depolymerization of Kraft Lignin with In-Situ H2. *Bioresour. Technol.* **2018**, *264* (March), 1−6.
(59) Fu, Z.-P.; Zhao, Y.-P.; Wu, F.-P.; Xie, J.-X.; Qiu, L.-L.; Xiao, J.; Liang, J.; Bai, Y.-H.; Liu, F.-J.; Cao, J.-P. Selective Hydrogenolysis of C-O Bonds in Lignin Model Compounds and Kraft Lignin over Highly Efficient NixCoyAl Catalysts. *Mol. Catal.* **2023**, *547*, 113334.
(60) Li, J.; Sun, H.; Liu, J.; Zhang, J.; Li, Z.; Fu, Y. Selective Reductive Cleavage of C O Bond in Lignin Model Compounds over Nitrogen-Doped Carbon-Supported Iron Catalysts. *Mol. Catal.* **2018**, *452*, 36−45.
(61) Kozuch, S.; Martin, J. M. L. Turning Over" Definitions in Catalytic Cycles. *ACS Catal.* **2012**, *2* (12), 2787−2794.

https://doi.org/10.1021/acscatal.4c06058
ACS Catal. 2025, 15, 1182−1194